Probing the interfacial adhesion strength in compositional libraries of epoxy films

Christopher M. Stafford, Jae Hyun Kim, Daisuke Kawaguchi,[1] Gareth Royston,[2] and Martin Y.M. Chiang
Polymers Division, National Institute of Standards and Technology
Gaithersburg, MD 20899-8542, U.S.A.
[1] Nagoya University, Nagoya, Japan
[2] University of Sheffield, Sheffield, UK

ABSTRACT

We are developing a measurement platform, based on the edge delamination test geometry, geared towards combinatorial and high-throughput (C&HT) assessment of interfacial adhesion and reliability of epoxy films bonded to a rigid substrate. A critical parameter space to be explored is composition of the epoxy formulation. We have constructed an automated mixing and deposition system for creating discrete and continuous gradients in composition of viscous epoxy formulations. By dicing the combinatorial library into a contiguous discrete sample array, the interfacial adhesion strength can be deduced from the critical stress required to debond each film cell from the substrate. These results can be used to predict the adhesion reliability of epoxy formulations as a function of composition and applied stress.

INTRODUCTION

Considerable attention has been devoted to developing high-throughput measurements for characterizing the chemical properties of combinatorial polymer libraries.[1,2,3,4] Less attention has been dedicated to designing high-throughput metrologies for probing the physical or engineering properties of combinatorial polymer libraries.[5,6,7,8] Our research aims to demonstrate and validate successful integration of suitable C&HT methodologies into new or existing measurement platforms for the physical testing of materials, with an emphasis in the areas of adhesion and mechanical properties. For example, at the NIST Combinatorial Methods Center (NCMC)[9] we have designed, developed, and demonstrated a combinatorial approach to the edge delamination test[10,11] to characterize the adhesion of thin polymer films.[12,13] This multivariant test is based on

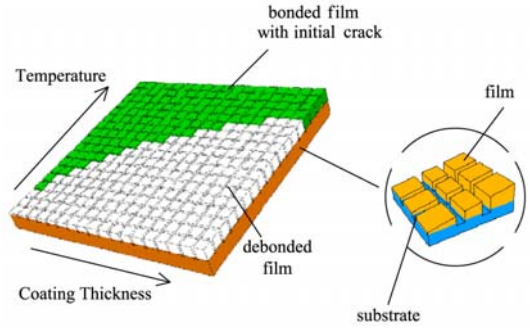

Figure 1. Schematic of the combinatorial edge delamination test for probing interfacial adhesion strength.

fracture of a film/substrate interface possessing an initial interfacial crack at a stress-free edge. To fabricate a specimen for the combinatorial edge delamination test, the film/substrate bi-layer is diced into squares approximately (1 to 2) cm^2 using a wafer saw or similar technique (see Figure 1). The dicing process initiates small defects (cracks) between the film and substrate. Upon cooling the specimen, crack extension (debonding) is driven by stresses generated at the crack tip brought about by the coefficient of thermal expansion (CTE) mismatch between the two materials. At a certain critical stress, the adhesion at the interface fails and the crack propagates from the edge of the sample towards the center. This metrology provides a rapid screen for interfacial reliability of a wide variety of bi-materials systems, particularly glassy and thermoset polymeric materials.

Previous research on the combinatorial edge delamination test focused on applying gradients in thickness of the film, surface energy of the substrate, and temperature.[12,13] There would be considerable value in incorporating compositional gradients into this measurement platform. Optimization of material properties of a multi-component material requires time-consuming formulation and exhaustive testing. High-throughput screening offers rapid assessment of new candidate materials and can define appropriate operating windows and tolerances, based on new material suppliers, new formulations, and/or changes in processing conditions. Therefore, we are pursuing methods for depositing compositional gradients of viscous formulations in appropriate library geometries for the combinatorial edge delamination test. Figure 2 shows a schematic of compositional libraries of polymeric film/substrate that will be discussed in this study. While the deposition system is generically applicable to any substrate/formulation combination, this study focuses on the adhesion of epoxy libraries to copper substrates geared to semiconductor packaging applications.

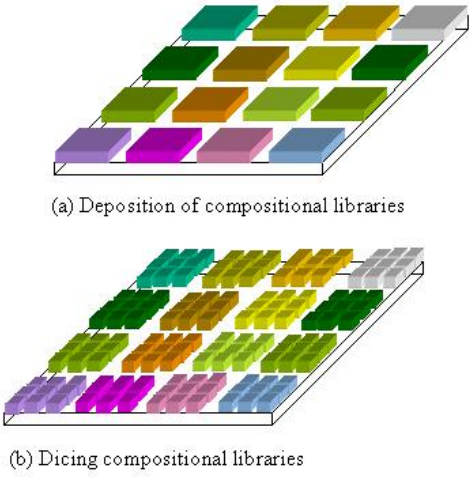

Figure 2. Geometry employed for generating compositional libraries of epoxy formulations (a) before and (b) after dicing.

EXPERIMENTAL DETAILS[14]

Materials. The epoxy system studied in this work consisted of 3,4-epoxy cyclohexyl methyl-3,4-epoxy cyclohexyl carboxylate (epoxy resin), hexahydro-4-methylphthalic anhydride (curing agent), and cobalt (III) acetylacetonate (catalyst). These chemicals were purchased from Aldrich and used as received. The copper plates were purchased from Prototype & Shortrun Services, Inc. (Fullerton, CA) and were polished by the supplier to an rms roughness of 1 μm. The surface oxide on the copper plates was removed by treatment with 1 % by mass solution of sulfuric acid in water followed by 1 % by mass solution of benzotriazole in water. The copper plates were used immediately after this cleaning procedure to minimize the re-oxidation of the surface.

From the atomic force microscope (AFM) height image, the surface of the copper plates has pits of up to 300 nm depth. However, the optical micrograph below shows that these defects are distributed widely and randomly about the surface on length scales much smaller than the 5 mm square sample size. Therefore, variations in surface roughness between samples were ignored.

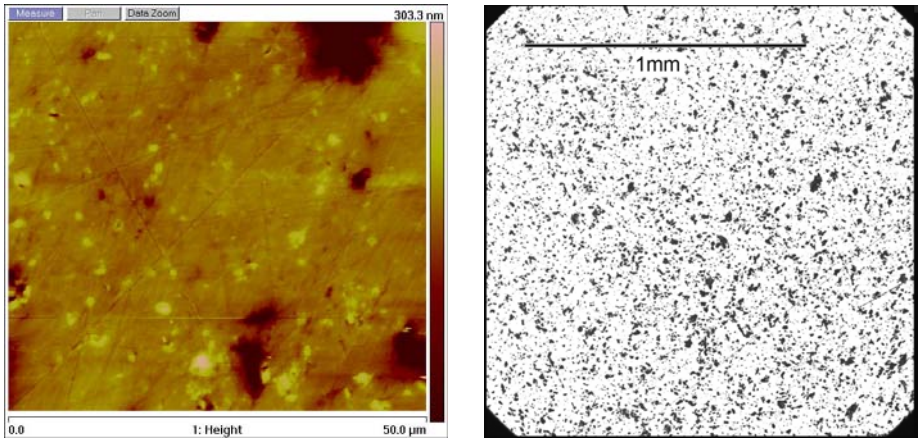

Figure 3. (Left) AFM height image and (right) optical microscope image of the copper plates. The AFM image is 50 μm × 50 μm with a height of 300 nm. The scale bar in the optical image is 1 mm.

DISCUSSION

Deposition system for compositional gradient. Compositional gradients of epoxy resin are generated using the meter/mix/dispense system shown in Figure 4. This deposition system consists of two computer-controlled syringe pumps, a static mixer, and an *x-y* translation stage for placement of the epoxy mixture on a substrate. Epoxy resin and catalyst are pre-mixed and loaded into one syringe pump, while the curing agent is loaded into a second syringe pump. A LabView interface is used to send commands to the syringe pumps. By varying the ratio of pumping speeds, the composition of the stream can be tuned either in a discrete fashion or continuously. In all examples discussed here, discrete gradients in composition are generated on copper substrates using various protocols for defining the array size and spacing.

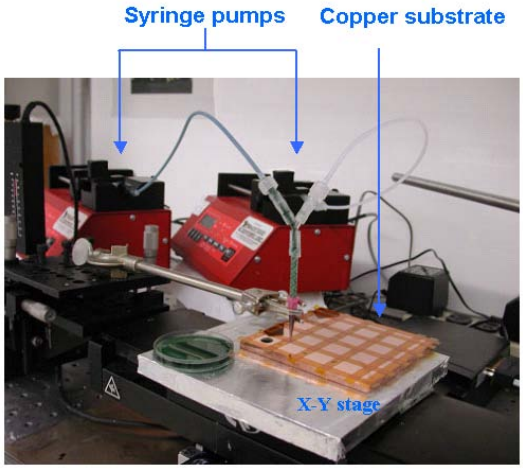

Figure 4. Deposition system for metering, mixing, and deposition of composition gradients of viscous polymer formulations.

The accuracy and repeatability of the deposition system was checked via gravimetrics. A lab balance was placed under the substrate being coated, and the accumulated weight of the deposited droplets was recorded. As shown in Figure 5, the deposition system reproducibly meters out the same amount of material in each drop. The current volume of one fresh epoxy drop is roughly ≈ 0.1 mL and accumulated mass of epoxy/curing agent exhibits a linear dependence on the number of deposited droplets on the substrate.

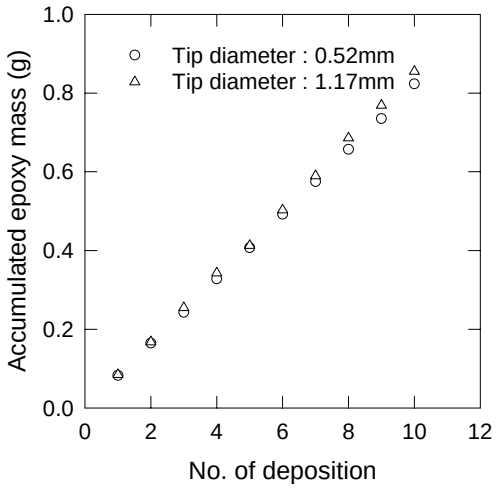

Figure 5. Accumulated mass of epoxy as a function of the number of drops deposited on the substrate.

Epoxy Libraries. The deposition system can dispense an array of droplets onto the copper plate. This droplet array can be used as-is or can be spread out to form a corresponding array of film specimens. An example of an 8×8 array of droplets is shown in Figure 6(a), where the array spacing is 1 cm in both directions. Alternatively, the droplet array can be spread out to form a film prior to curing. Currently, this is achieved using a draw-down process similar to doctor blading, but we are exploring different spreader tip geometries that would allow film formation to be achieved in a more

(a) (b)

Figure 6. (a) Discrete array of 8×8 droplets deposited onto copper, and (b) array of 4×4 individual films created by spreading of a discrete array of droplets. The droplet arrays were deposited using the deposition system shown in Figure 4.

automated fashion. Figure 6(b) shows compositional libraries of epoxy films (thickness ≈ 90 μm) on a copper substrate generated by this draw-down process. The un-cured film thickness is pre-determined through the use of adhesive Kapton film spacers.

After deposition, the epoxy is cured at 170 °C for 2 h. In the droplet geometry, it is critical that the curing oven be level to minimize the flow or smearing of the epoxy droplets during curing. Figure 7(a) shows the droplet array after curing, while Figure 7(b) shows the film array after curing. The composition of each droplet changes gradually from the bottom right corner to the upper left corner, as labeled in the figure. Currently, we are pursuing high-throughput spectroscopic methods for verifying the composition and homogeneity of each droplet in the array.

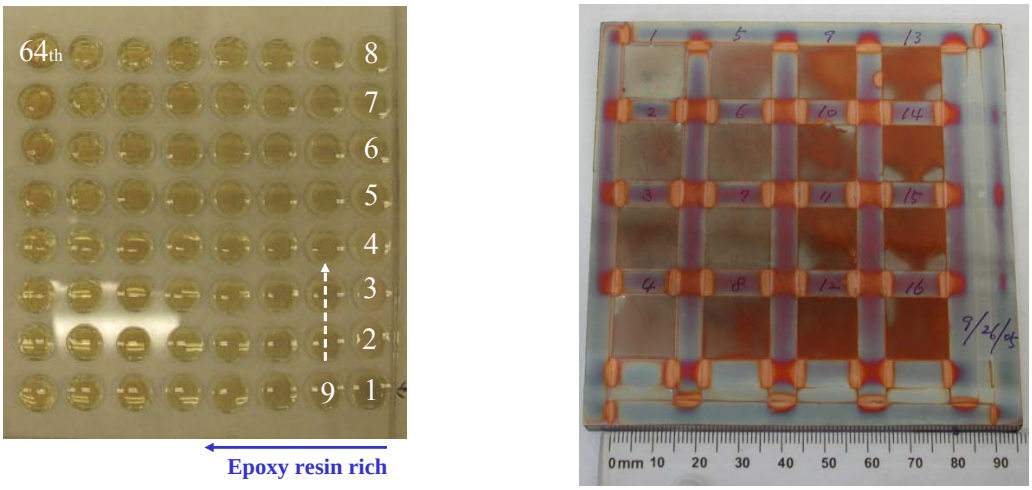

(a) (b)

Figure 7. (a) Droplet array and (b) film array of compositional gradients of epoxy formulation after curing at 170 °C for 2 h.

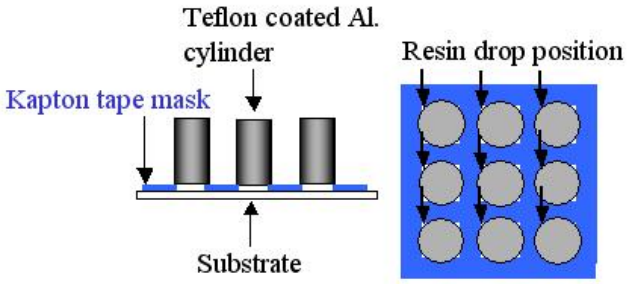

(a)

(b)

Figure 8. (a) Schematic of the closed molding technique using a capillary force and (b) an image of a specimen generated using this technique.

We are also pursuing a closed molding technique for generating epoxy films of controllable and uniform thickness. A schematic of this technique is shown in Figure 8(a). In this technique, an adhesive Kapton film mask is placed on the substrate, where the mask determines the final thickness of the cured epoxy films. Next, Teflon AF-coated aluminum cylinders are placed on the Kapton mask to provide a confining wall. Then an epoxy droplet is deposited adjacent to the Al cylinders such that capillary forces pull the epoxy into the gap between the substrate and the cylinder. This process is self-metering in that the droplet volume can greatly exceed the volume of the gap, but only the minimal volume of epoxy is pulled under the cylinder. The epoxy resin is cured while confined by the aluminum cylinders, resulting in a uniform thickness of epoxy film as shown in Figure 8(b). This technique is only applicable for formulations without volatile components; if solvents are present, it will lead to void formation in the film during curing under confinement.

Debonding of Epoxy Libraries. The epoxy libraries are subsequently exposed to cryogenic temperatures to drive the debonding process. This is due to the mismatch in the coefficients of thermal expansion between the film and substrate, which results in a net biaxial stress at the interface that drives crack propagation and failure. An example of this process is shown in Figure 9, where a compositional gradient film array similar to that shown in Figure 7(b) was quenched to -150 ^{o}C to induce debonding. The numbers above each cell correspond to a specific composition of epoxy deposited in that cell. A quick visual inspection reveals that the film in cell #7 has inadequate adhesion to the copper substrate, while the film in cell #16 exhibits good adhesion to the substrate.

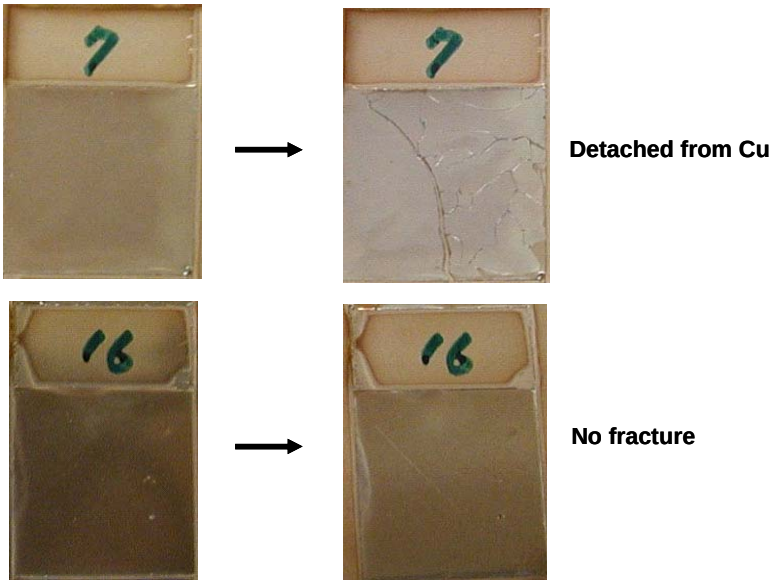

Figure 9. Examples of debonded (top) and bonded (bottom) epoxy films after quenching to -150 ^{o}C. The numbers above each film correspond to specific compositions of epoxy formulation dispensed into that particular cell of the film array.

CONCLUSIONS

We have developed the framework for a combinatorial approach for mapping the interfacial reliability of a thin polymer films based on the edge delamination test geometry. This approach relies on the use of gradient techniques to create a multivariant sample that spans a parameter space previously achieved by creating multiple individual samples. We constructed and demonstrated an automated mixing and deposition system for the creation of discrete gradients in composition of a thermally cured epoxy system. The discrete gradient array can be constructed in the form of droplets or films, depending on the application requirements. Debonding of the compositional gradient array is induced by quenching the bi-material system to cryogenic temperatures. A qualitative visual assessment reveals the compositional space where interfacial adhesion is sufficient and where the film debonds from the substrate.

FUTURE WORK

As we continue to develop this combinatorial metrology, a key element to the library fabrication step is dicing of the film array into multiple independent delamination specimens. Dicing of the sample is performed on an automated wafer dicing saw, and an example of a diced film array is shown in Figure 10. As a result, each square (15 mm × 15 mm) consists of 4+ specimens (5 mm × 5 mm) within each compositional cell. The cut penetrates some distance (≈ 40 μm) into the substrate and forms 90° edges at the film/substrate interface. The dicing process results in a clean free edge with reproducible pre-crack lengths. This process also provides replicate samples for each composition for generating proper statistical data.

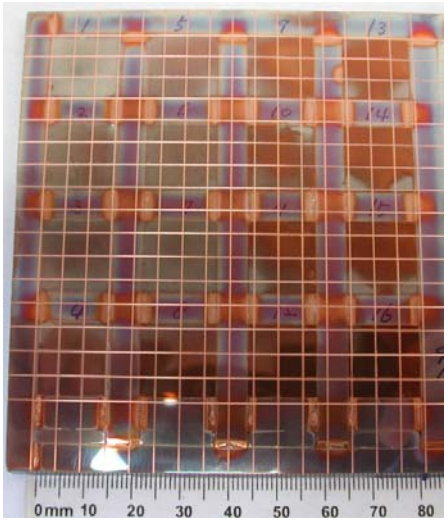

Figure 10. Example of a diced film array similar to Figure 7(b). Dicing the film array affords a well defined pre-crack and free edge as well as provides replicate samples within each compositional cell.

We are also currently measuring the representative mechanical properties of this epoxy system in order to quantify the interfacial fracture toughness. During the debonding of a film, if the fracture toughness in an opening mode (K_{IC}) is assumed to be the major driving force for debonding in the edge delamination test, it can be expressed as follows:[11,12]

$$K_{IC} = \sigma_0 \sqrt{\frac{h_f}{2}} \tag{1}$$

where σ_0 is the internal biaxial stress that depends on the thermal mismatch, and h_f is the thickness of film. σ_0 can be calculated through the material's stress-temperature relationship, as determined by wafer curvature measurements,[12] or if the mechanical properties of the film and substrate are known, σ_0 is calculated using the following equation:

$$\sigma_0 = \overline{E}_f (\alpha_s - \alpha_f)(T - T_{ref}) \tag{2}$$

where

$$\overline{E}_f = \frac{E_f}{1 - \nu_f} \tag{3}$$

and E and α are the elastic modulus and coefficients of the thermal expansion, respectively. The subscripts f and s represent the film and substrate, respectively. T_{ref} is the reference temperature, which can be taken as the T_g of the film. From this stress-temperature relationship between a film and a rigid substrate, a quick estimation of the stress is achieved. For a failure mode other than pure opening, the analysis procedures should be identical with the exception that Equation 1 should be replaced by a more appropriate expression (i.e., one that includes mixed mode behavior).

ACKNOWLEDGMENTS

Contribution of the National Institute of Standards and Technology, not subject to copyright in the United States. GR would like to thank the Society of Chemical Industry (Messel Bursary) and InsightFaraday for financial assistance. GR also thanks Dr. J. Patrick A. Fairclough for help and support. The support of ICI - National Starch & Chemical and Intel is gratefully acknowledged.

REFERENCES

[1] Hoogenboom, R., and Schubert, U. S., *Rev. Sci. Instrum.* **76**, 062202 (2005).
[2] Zhang, H., Hoogenboom, R., Meier, M. A. R., Schubert, U. S. *Meas. Sci. Technol.* **16**, 203 (2005).
[3] Genzer, J. *J. Adhes.* **81**, 417 (2005).
[4] Cygan, Z. T., Cabral, J. T., Beers, K. L., Amis, E. J. *Langmuir* **21**, 3629 (2005).
[5] Chisholm, B., Potyrailo, R., Cawse, J., Shaffer, R., Brennan, M., Molaison, C., Whisenhunt, D., Flanagan, B., Olson, D., Akhave, J., Saunders, D., Mehrabi, A., Licon, M. *Prog. Org. Coat.* **45**, 313 (2002).
[6] Grunlan, J. C., Holquin, D. L., Chuang, H. K., Perez, I., Chavira, A., Quilatan, R., Akhave, J., Mehrabi, A.R. *Macromol. Rapid Comm.* **25**, 286, (2004).
[7] Sormana, J. L., Chattopadhyay, S., Meredith, J. C. *Rev. Sci. Instrum.* **76**, 062214 (2005).
[8] Kossuth, M. B., Hajduk, D. A., Freitag, C., Varni, J. *Macromol. Rapid Comm.* **25**, 243 (2004).
[9] http://www.nist.gov/combi
[10] Farris, R. J., Bauer, C. L. *J. Adhes.* **26**, 293 (1988).
[11] Shaffer, E. O., McGarry, F. J., Hoang, L. *Polym. Eng. Sci.* **36**, 2375 (1996).
[12] Chiang, M. Y. M., Wu, W. L., He, J. M. Amis, E. J. *Thin Solid Films* **437**, 197 (2003).
[13] Chiang, M. Y. M., Song, R., Crosby, A. J., Karim, A., Chiang, C. K., Amis, E. J. *Thin Solid Films* **476**, 379 (2005).
[14] Certain equipment, instruments or materials are identified in this paper in order to adequately specify the experimental details. Such identification does not imply recommendation by the National Institute of Standards and Technology nor does it imply the materials are necessarily the best available for the purpose.